Chemical Science

ROYAL SOCIETY OF CHEMISTRY

EDGE ARTICLE

View Article Online
View Journal | View Issue

Check for updates

Cite this: *Chem. Sci.*, 2025, **16**, 22701

All publication charges for this article have been paid for by the Royal Society of Chemistry

Received 5th June 2025
Accepted 21st October 2025

DOI: 10.1039/d5sc04074d

rsc.li/chemical-science

Diselenide-enabled photocatalytic hydroazolation of *gem*-difluoroalkenes

Mohammed K. Abd El-Gaber, †[abc] Ryan M. Herrick, †[a] Pranaya Sudhakar, [d] Ashutosh Rana, [e] Brent A. Roach, [e] Jeffrey E. Dick [ef] and Ryan A. Altman *[ae]

Difluoromethylene-containing molecules and azoles, independently, have wide applications in materials science, pharmaceuticals, agrochemicals and as biological diagnostic probes. However, compounds bearing the *N*-α,α-difluoroalkyl azole [(azole)N–CF_2R] motif remain scarce in academic and patent literature, presumably due to a lack of synthetic methods. Such compounds could be convergently accessed in a single step *via* the hydroazolation of *gem*-difluoroalkenes. However, most existing functionalization reactions of *gem*-difluoroalkenes proceed through a β-fluoride elimination pathway that generates monofluorinated derivatives. Herein, we report a photocatalytic hydroazolation of *gem*-difluoroalkenes to generate (azole)N–CF_2R that employs an uncommon diselenide co-catalyst to avoid the defluorinative process, ultimately enabling facile access to underexplored medicinally and agriculturally-relevant chemical space.

Introduction

N-Heterocycles and fluorinated motifs are two frequently encountered substructures with applications in materials science, medicinal chemistry, agricultural chemistry, and as diagnostic probes.[1–3] Strategies that enable access to novel and/or underrepresented combinations of these substructures have the potential to impact a variety of applied fields. One such combination, *N*-α,α-difluoroalkyl azoles [(azole)N–CF_2R, **1**, Scheme 1A], have displayed medicinal potential in neurodegenerative disease,[4,5] oncology,[6] and inflammation.[7,8] Notwithstanding these examples, (azole)N–CF_2R remain underutilized in medicinal and agricultural chemistry (<30 compounds with experimentally determined pharmacological activity for R = alkyl, SciFinder, Octcober 2025). This deficiency represents a missed opportunity to explore biologically relevant chemical space, as the perturbations of molecular physicochemical properties imparted by fluorine on (azole)N–CF_2R containing compounds presumably mimic those observed for *N*-trifluoromethyl azoles [(azole)N–CF_3], a more common *N*-fluoroalkyl azole substructure in medicinal chemistry.[9–14] Specifically, (azole)N–CF_3 possess decreased pK_a, increased lipophilicity, and greater stability towards metabolic *N*-dealkylation relative to their non-fluorinated counterparts.[11,15] Despite these attributes, the trifluoromethyl group precludes further growth of a ligand off the azole's nitrogen atom in (azole)N–CF_3. In contrast, the (azole)N–CF_2R substructure could benefit from fluorine-induced perturbations while also allowing for elaboration of the *N*-alkyl group.

The underutilization of the (azole)N–CF_2R group can be partially attributed to the lack of viable synthetic methods to access this moiety. Existing methods for azole *N*-fluoroalkylation typically form *N*-fluoromethyl azoles[16,17] or higher order *N*-perfluoroalkyl azoles (*e.g.*, C_2F_4, C_3F_6)[18,19] – few strategies exist for generating simple, hydrocarbon (azole)N–CF_2R.[20–22] To access this substructure, an attractive retrosynthetic disconnection across the N–CF_2 bond might reveal *gem*-difluoroalkene (**2**)[23–28] and azole (**3**) synthons, two readily accessible substrates (Scheme 1A). In the forward reaction, regioselective C–N bond formation would occur through attack of the azole at the electrophilic difluorinated carbon of **2**.[29,30] Indeed, azole nucleophiles do react with 3,3-difluoropropen-1-yl ammonium salt **4** to generate *N*-*gem*-difluoroallyl azoles (**5**) by an S_N2' process in the presence of stoichiometric NaH (Scheme 1B).[31] However, the singular *gem*-difluoroalkene coupling partner prevents this reaction from serving as a convergent approach to generate a diverse array of (azole)N–CF_2R.

In the absence of a quaternary ammonium leaving group, base-mediated nucleophilic addition of azoles to *gem*-difluoroalkenes proceeds through an unstable anionic

[a]*Borch Department of Medicinal Chemistry and Molecular Pharmacology, Purdue University, West Lafayette, IN 47907, USA. E-mail: raaltman@purdue.edu*

[b]*Medicinal Chemistry Department, Faculty of Pharmacy, Assiut University, Assiut 71526, Egypt*

[c]*Department of Pharmaceutical Sciences, University of Tennessee Health Science Center, Memphis, TN 38163, USA*

[d]*Department of Biology, Purdue University, West Lafayette, IN 47907, USA*

[e]*James Tarpo Jr and Margaret Tarpo Department of Chemistry, Purdue University, West Lafayette, IN 47907, USA*

[f]*Elmore Family School of Electrical and Computer Engineering, Purdue University, West Lafayette, IN 47907, USA*

† These authors contributed equally to this work.

Open Access Article. Published on 21 October 2025. Downloaded on 6/12/2026 4:04:08 PM. This article is licensed under a Creative Commons Attribution-NonCommercial 3.0 Unported Licence.

Open Access Article. Published on 21 October 2025. Downloaded on 6/12/2026 4:04:08 PM.
This article is licensed under a Creative Commons Attribution-NonCommercial 3.0 Unported Licence.

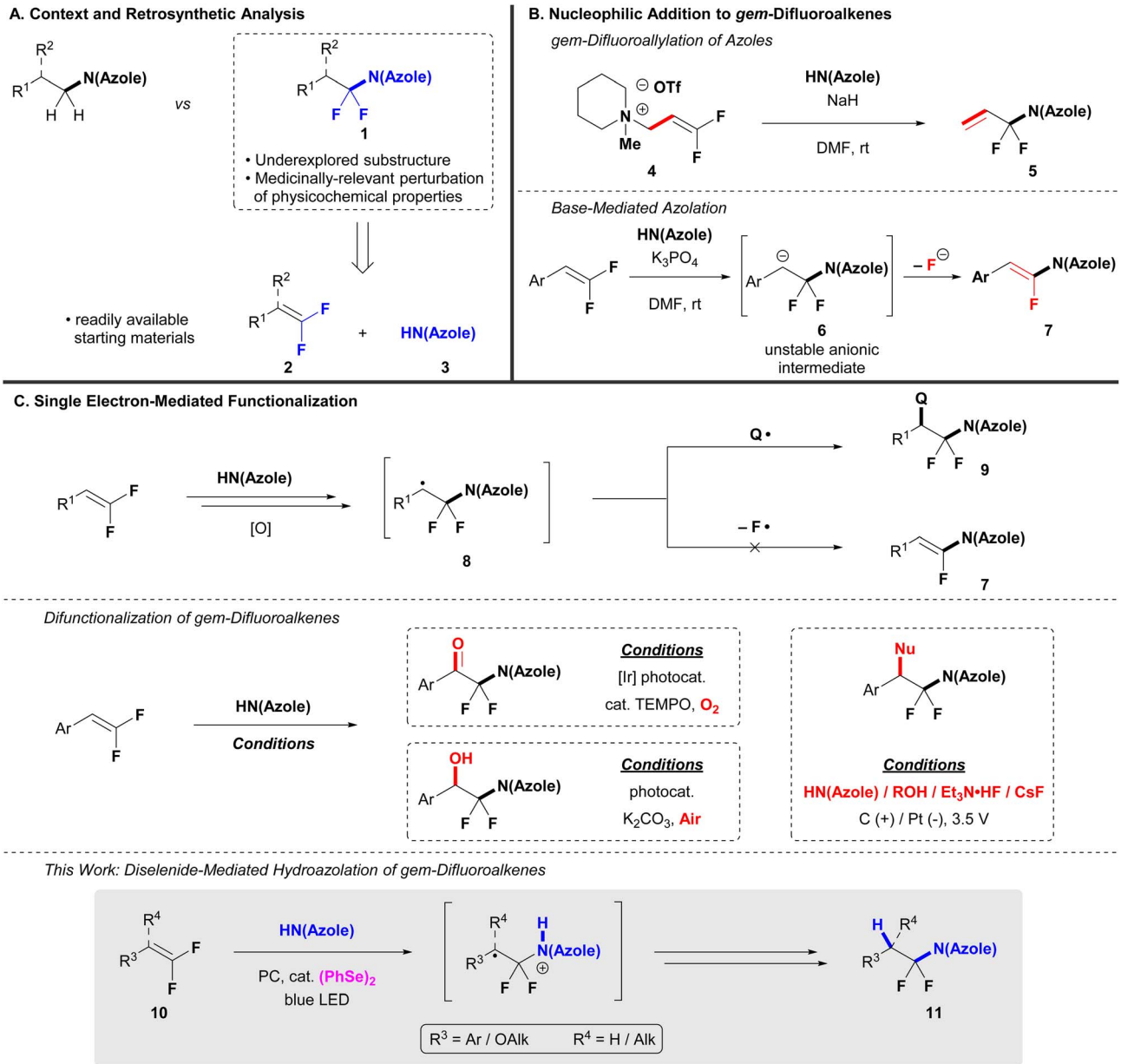

Scheme 1 Accessing (azole)N–CF_2R: azolation of *gem*-difluoroalkenes.

intermediate **6** that readily loses a β-fluoride anion to form *N*-(α-fluorovinyl) azoles (**7**, Scheme 1B),[29,32,33] not (azole)N–CF_2R. Alternatively, single electron-mediated azolation of *gem*-difluoroalkenes represents a strategy that could circumvent the limitations of β-fluoride elimination and the necessity for specialized *gem*-difluoroalkene coupling partners (Scheme 1C). Specifically, the addition of azoles to diverse *gem*-difluoroalkenes under oxidative conditions generates a radical intermediate **8** that could be quenched by an appropriate radical source, thus avoiding anionic intermediate **6** and fluoride elimination.[29] Such reactions of *gem*-difluoroalkenes have been accomplished using photocatalysts and electrolytic cells as single-electron oxidants to promote difunctionalization reactions that add azoles with O_2,[34,35] fluoride,[36,37] alcohols, and an additional azole molecule (Scheme 1C).[38] However, a simple hydrofunctionalization of *gem*-difluoroalkenes with azoles to form (azole)N–CF_2R remains elusive.

To address this synthetic deficiency, we herein disclose a diselenide-mediated photocatalytic hydroazolation of *gem*-difluoroalkenes with both monocyclic and benzannulated azoles that delivers previously unreported (azole)N–CF_2R. In this reaction, the diselenide co-catalyst promotes the desired hydrofunctionalization process and avoids undesired reactivity with *gem*-difluoroalkenes, similarly to a hydroalkoxylation reaction of *gem*-difluoroalkenes previously reported by our group.[44] However, amongst a series of tested dichalcogenide co-catalysts, $(PhSe)_2$ uniquely reversed selectivity for defluorinative azolation. Additionally, experimental data supports

© 2025 The Author(s). Published by the Royal Society of Chemistry

Open Access Article. Published on 21 October 2025. Downloaded on 6/12/2026 4:04:08 PM. This article is licensed under a Creative Commons Attribution-NonCommercial 3.0 Unported Licence.

a mechanism initiated by direct photocatalyst oxidation of *gem*-difluoroalkenes, which contrasts the previous report.[44]

By merging two commonly exploited substructures found in biologically active compounds (azoles and fluoroalkyl groups), this approach opens numerous possibilities for expanding the synthetically accessible chemical space that could impact the development of therapeutics, biological probes, agrochemical agents, and materials.

Results and discussion

In the initial reaction design, we aimed to generate azole radicals that would react with *gem*-difluoroalkenes to afford carbon-centered radical intermediate **8**, which, after quenching by a hydrogen atom transfer (HAT) step, would deliver the desired (azole)N–CF_2R (**11**). This strategy was inspired by previous reports of *gem*-difluoroalkene hydrothiolation that are initiated by a photocatalyst-mediated oxidation/PCET of thiols that generates thiyl radicals.[45–47] To test this hypothesis, photocatalysts spanning a range of excited state reduction potentials were reacted with benzimidazole and electron-rich *gem*-difluorostyrene **10a** as model substrates on a 50 μmol scale (Table 1, entries 1–6). Conversion of the *gem*-difluorostyrene occurred only when photocatalysts with excited state reduction potentials greater than +0.45 V were employed; however, only trace product formed (entries 4–6). Instead, these reactions formed monofluorovinyl azole side-product **12**, suggesting that the system lacked an adequate hydrogen atom source to quench presumed radical intermediate **8** (see Scheme S5 for a mechanistic proposal for the formation of side-products **12** and **13**). Initial attempts to identify catalytic additives that could donate hydrogen atoms and generate desired product **11aa** (*e.g.*, arylamines, *N*-hydroxyphthalimide (NHP), silanes, and thiols) failed to increase selectivity for the desired (azole)N–CF_2R **11aa** (entries 7–10). However, dichalcogenide additives improved the reaction (entries 11–14), with the best yield and selectivity observed with $(PhSe)_2$ (entry 14). Notably, $(PhSe)_2$ was not consumed by a hydroselenolation side-reaction with *gem*-difluorostyrene **10a**, which distinguishes the diselenide from a more common disulfide additive (entry 11).[48,49] Reduction of $(PhSe)_2$ loading from 20% to 5% further improved reaction performance (entry 15). Final optimization on a 0.50 mmol scale revealed optimal loadings of reagents [1.2 equiv. azole, 5%

Table 1 Reaction optimization[a]

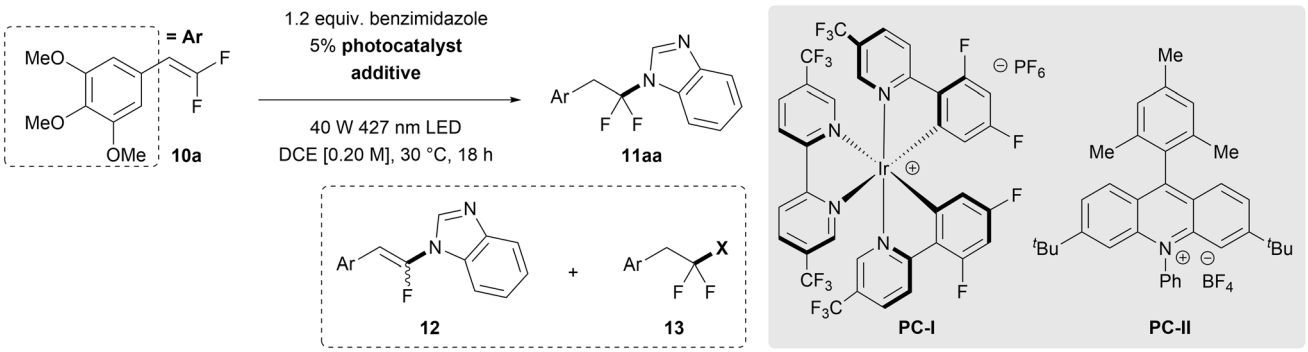

Entry	Photocatalyst	$E_{1/2}$ [PC*^{n}/PC^{n-1}] (V *vs.* Fc/Fc$^+$)[b]	Additive	% Conv. **10a**	% Yield **11aa**	%Yield **12**	% Yield **13**
1	$[Ir(dtbbpy)(ppy)_2]PF_6$	+0.28 (ref. 39)	None	<5	0	0	N.D.[d]
2	Rose Bengal lactone	+0.28 (ref. 40)	None	<5	0	0	N.D.[d]
3	Eosin Y (dibasic)	+0.45 (ref. 40)	None	<5	0	0	N.D.[d]
4	4CzIPN	+1.00 (ref. 40)	None	67	<1	66	N.D.[d]
5	**PC-I**	+1.30 (ref. 41)	None	69	5	64	N.D.[d]
6	**PC-II**	+1.70 (ref. 42)	None	66	<1	64	N.D.[d]
7	**PC-I**	+1.30 (ref. 41)	*m*-Anisidine (10%)	61	3	56	0
8	**PC-I**	+1.30 (ref. 41)	TRIP-SH (30%)[c]	53	3	44	0
9	**PC-I**	+1.30 (ref. 41)	NHP (50%)[c]	72	<1	66	0
10	**PC-I**	+1.30 (ref. 41)	$(TMS)_3SiH$ (50%)	70	8	56	0
11	**PC-I**	+1.30 (ref. 41)	$(PhS)_2$ (20%)	>99	26	42	17 (X = SPh)
12	**PC-I**	+1.30 (ref. 41)	$(BnS)_2$ (20%)	81	4	68	0
13	**PC-I**	+1.30 (ref. 41)	$(BnSe)_2$ (20%)	82	21	44	<1 (X = F)
14	**PC-I**	+1.30 (ref. 41)	$(PhSe)_2$ (20%)	>99	81	4	2 (X = F)
15	**PC-I**	+1.30 (ref. 41)	$(PhSe)_2$ (5%)	>99	93	0	0

[a] Reaction conditions: *gem*-difluorostyrene **10a** (50 μmol), benzimidazole (1.2 equiv.), additive, and photocatalyst (5 mol%) in DCE (0.25 mL) irradiated with a 40 W 427 nm LED under an atmosphere of N_2. Conversion and yields were determined by ^{19}F NMR using (trifluoromethyl) benzene as an internal standard. [b] Literature-reported reduction potentials were corrected to the Fc/Fc$^+$ redox couple.[43] [c] TRIP-SH = 2,4,6-triisopropylbenzenethiol, NHP = *N*-hydroxyphthalimide. [d] N.D. = not detected.

Open Access Article. Published on 21 October 2025. Downloaded on 6/12/2026 4:04:08 PM. This article is licensed under a Creative Commons Attribution-NonCommercial 3.0 Unported Licence.

$(PhSe)_2$, and 5% **PC-I**], solvent (DCE, Table S2), and concentration (0.25 M). Additionally, while the presence of H_2O (up to 1 equiv.) had no deleterious effect on the reaction, O_2 was detrimental. In parallel efforts, an alternate set of conditions derived from a previously reported *gem*-difluoroalkene hydroalkoxylation reaction[44] were developed for the more strongly oxidizing **PC-II** [1.2 equiv. azole, 5% $(PhSe)_2$, 3% **PC-II**, 0.25 M PhMe, Table S4] and would eventually be essential for certain substrates. Control experiments verified that photocatalyst, visible light, and $(PhSe)_2$ were all necessary for successful hydroazolation of *gem*-difluorostyrenes (Table S1).

A range of azoles successfully reacted with *gem*-difluorostyrene **10a** using the optimized **PC-I** conditions (Table 2). Specifically, unsubstituted benzimidazole reacted to afford product **11aa** in 87% yield. 5-Monosubstituted benzimidazoles bearing electron-withdrawing –Cl, –Br, $–CO_2Me$, and $–NO_2$ groups reacted with moderate to excellent yield (**11ab–ae**, 40–91%). A mixture of *N*-regioisomers was generated, but the 6-substituted products predominated, for which the major regioisomer was assigned by a combination of X-ray crystallography (see Data availability on p. 8) and $^1H\{^{19}F\}$ Nuclear Overhauser Effect (NOE) NMR. Other benzannulated azoles, such as indazoles (**11af** and **11ag**, 92% and 61%) and benzotriazole (**11ah**, 96%) reacted with good yield and near exclusive regioselectivities. Notably, the high N2-regioselectivity for indazoles **11af** and **11ag** supports a process involving nucleophilic C–N bond formation from a neutral indazole molecule.[50] Additionally, the FDA-approved drugs theophylline and triclabendazole were reacted with these conditions (**11ai** and **11aj**, 43% and 86%). 7-Azaindoles also coupled successfully with slight alterations to the standard conditions, albeit in low yields and with long reaction times (**11ak** and **11al**, 13% and 20%, 46 h and 44 h). Interestingly, these reactions exhibit exclusive *N*-regioselectivity for functionalization at the pyridyl nitrogen rather than the indole nitrogen, which is consistent with the observed inability of indoles to react in this system. However, 6-, 5-, and 4-azaindoles do not achieve net hydrofunctionalization and instead form monofluorovinyl azaindole products (ArCH = CFN(azaindole), **7**).

Reactions of monocyclic pyrazoles bearing electron-withdrawing groups (4-Br and 4-CO_2Et, **11am** and **11ao**, 88% and 89% [H_2O required for **11ao**, see Notes section]), electron-donating groups (3,5-Me and 4-BPin, **11ap** and **11ar**, 91% and 88%), and sterically restrictive 3,5-disubstitution (**11ap** and **11aq**, 91% and 87%) all furnished products in excellent yields. Importantly, the reaction's ability to tolerate bromide (**11am**, 88%), iodide (**11an**, 74% [H_2O required, see Notes section]), and boronate ester (**11ar**, 88%) substituents enables further

Table 2 Scope of azole substrates[a]

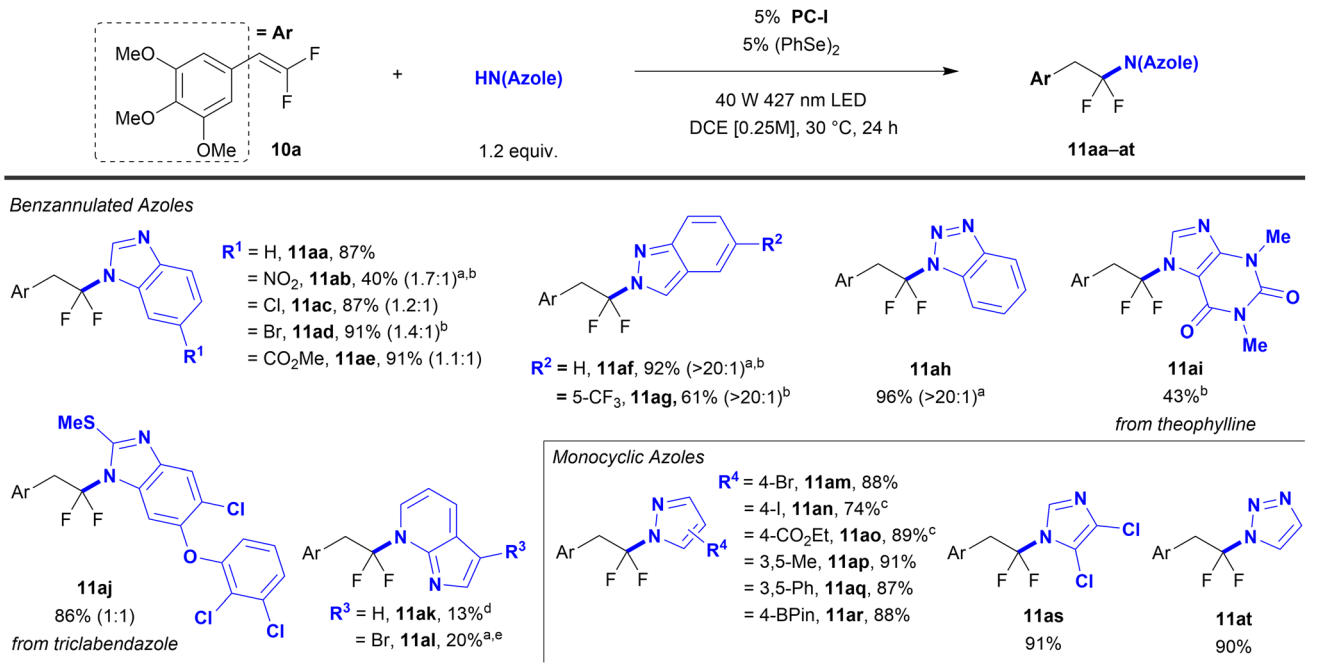

[a] Reaction conditions unless otherwise noted: *gem*-difluorostyrene **10a** (0.50 mmol), azole (1.2 equiv.), 1,2-diphenyldiselane (5 mol%), and **PC-I**: {Ir[dF(CF$_3$)ppy]$_2$-(5,5′-dCF$_3$bpy)}PF$_6$ (5 mol%) in DCE (2.0 mL) irradiated with a 40 W 427 nm LED under an atmosphere of N_2. Isolated yields represent an average of two independent reactions. Ratios in parentheses represent the major and minor *N*-regioisomeric ratio of the crude reaction mixture as determined by ^{19}F NMR. [b] Structure of the major product was assigned by X-ray crystallography (see Data availability on p. 8). [c] Structure of the major product was assigned by $^1H\{^{19}F\}$ NOE. [d] Reaction contained N_2-sparged H_2O (0.50 equiv.). [e] With 7-azaindole (1.5 equiv.), 1,2-diphenyldiselane (15 mol%), and **PC-I**: {Ir[dF(CF$_3$)ppy]$_2$-(5,5′-dCF$_3$bpy)}PF$_6$ (1 mol%) for 46 h. [f] With 1,2-diphenyldiselane (25 mol%) and **PC-II**: 9-mesityl-3,6-di-*tert*-butyl-10-phenylacridinium tetrafluoroborate (3 mol%) in PhMe (2.0 mL) for 44 h.

© 2025 The Author(s). Published by the Royal Society of Chemistry

Open Access Article. Published on 21 October 2025. Downloaded on 6/12/2026 4:04:08 PM. This article is licensed under a Creative Commons Attribution-NonCommercial 3.0 Unported Licence.

divergent functionalization by cross-coupling reactions. 4,5-Dichloro-1*H*-imidazole was successfully coupled (**11as**, 91%), and 1,2,3-1*H*-triazole reacted with excellent yield and exclusive N1–regioselectivity (**11at**, 90%). While the reaction demonstrated a broad scope of azole coupling partners, some poor-performing and unreactive substrates were identified (Table S5).

Using pyrazole as a model substrate, a wide range of *gem*-difluoroalkenes coupled in moderate to excellent yields under either **PC-I** or **PC-II** catalysis (**11a–r**, 24–88%, Table 3). To select the appropriate photocatalyst for the reaction of each *gem*-difluoroalkene, conditions derived for **PC-I** and **PC-II** were preemptively screened on a 50 μmol scale (Table S6) and successful reactions were repeated on a 0.50 mmol scale. The reaction tolerated a range of heterocyclic *gem*-difluorostyrenes (**11b–f**, 41–86%), including pyrazoles, benzothiophenes, benzofurans, indoles, and pyrroles. Additionally, though a rarely reported glucose-derived difluorinated enol substrate (**10g**) reacted sluggishly with pyrazole (5 days to achieve ~50% yield on a 50 μmol scale), indazole successfully coupled with saccharide **10g** to generate a single diastereomer at C2 (**11g**, 44%, determined by X-ray crystallography, see Data availability on p. 8). Surprisingly, the N1-substituted indazole regioisomer predominated in this reaction (13 : 1 N1 : N2, determined by ^{19}F NMR and X-ray crystallography, see Data availability on p.8), which contrasts the coupling reactions of indazoles with *gem*-difluorostyrene **10a** (**11af** and **11ag**, Table 2) and *gem*-difluorostyrenes **10c**, **10e**, **10f**, and **10j** (Table S5) that display almost exclusive substitution at N2. Electronically neutral and rich *gem*-difluorostyrenes afforded moderate to high yields of *N*-α,α-difluoroalkyl pyrazoles (**11a**, **11j–p**, 57–88%). However, *gem*-difluorostyrenes with electron-withdrawing substituents reacted in lower yields and with slower conversion (**11q** and **11r**, 24% and 25%, 42 and 48 h). Notably, these substrates required the more strongly oxidizing acridinium-based photocatalyst (**PC-II** conditions) to generate detectable yields of the desired (azole)N–CF_2R products, a correlation that was not apparent for electronically neutral and rich substrates. Interestingly, neither *gem*-difluorostyrenes bearing strongly electron-withdrawing substituents (*e.g.*, 4-CN) nor aliphatic *gem*-difluoroalkenes reacted with azoles employing either **PC-I** or **PC-II** conditions (Table S6), which, supplemented by luminescence quenching studies and a comparison of substrate and photocatalyst redox potentials (see mechanistic discussion below), suggests that only *gem*-difluoroalkene substrates that can be oxidized by **PC-I** and **PC-II** will successfully react. Regardless, this limitation in

Table 3 Scope of *gem*-difluoroalkene substrates[a]

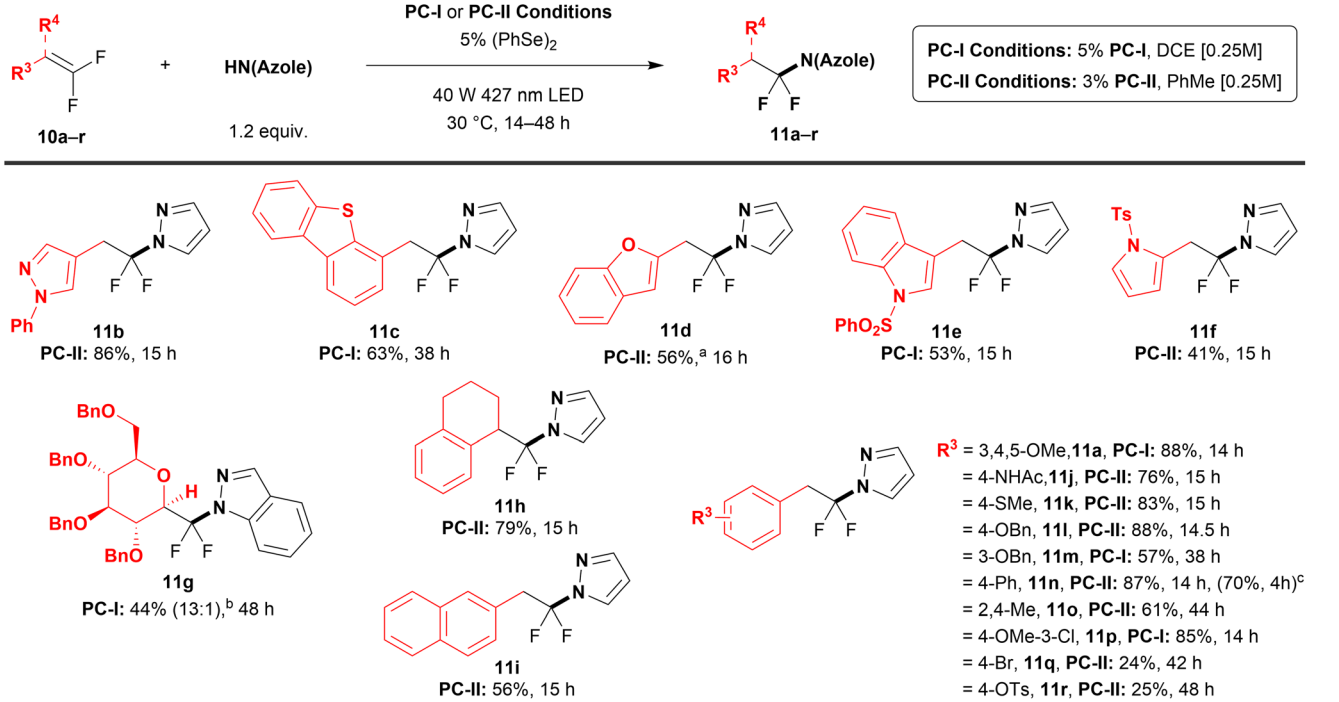

[a] Reaction conditions: *gem*-difluorostyrene **10a–r** (0.50 mmol), azole (1.2 equiv.), 1,2-diphenyldiselane (5 mol%), and either **PC-I**: {Ir[dF(CF_3)ppy]$_2$-(5,5′-dCF_3bpy)}PF_6 (5 mol%) in DCE (2.0 mL) or **PC-II**: 9-mesityl-3,6-di-*tert*-butyl-10-phenylacridinium tetrafluoroborate (3 mol%) in PhMe (2.0 mL) irradiated with a 40 W 427 nm LED under an atmosphere of N_2. Isolated yields represent an average of two independent reactions. [b] 15 mol% 1,2-diphenyldiselane was used. [c] Ratio represents the major and minor *N*-regioisomeric ratio of the crude reaction mixture as determined by ^{19}F NMR. Structure of the major product was assigned by X-ray crystallography (see Data availability on p. 8). [d] Data in parentheses: *gem*-difluorostyrene **10n** (4.6 mmol, 1.0 g), pyrazole (1.2 equiv.), 1,2-diphenyldiselane (5 mol%), and **PC-II** (3 mol%) in PhMe (18.5 mL) irradiated with a 40 W 427 nm LED under an atmosphere of argon. Isolated yield represents an average of two independent reactions.

Open Access Article. Published on 21 October 2025. Downloaded on 6/12/2026 4:04:08 PM. This article is licensed under a Creative Commons Attribution-NonCommercial 3.0 Unported Licence.

substrate scope contrasts a previously reported hydroalkoxylation method that utilizes a similar co-catalytic system.[44] Sterically hindered tetra-vinyl- and mono-*ortho*-substituted *gem*-difluorostyrene substrates reacted successfully (**11h** and **11o**, 79 and 61%); however, a 2,6-dimethyl *gem*-difluorostyrene could not be coupled (Table S6). Notably, the reaction was successful on a gram scale, albeit with modification to the photochemical reactor (see SI, S30) and worsened conversion efficiency (**11n**, 70% on 4.6 mmol scale *vs.* 87% on 0.5 mmol scale).

A combination of physicochemical data and literature precedent for photocatalyzed functionalization reactions of both nonfluorinated and *gem*-difluorinated alkenes supports a mechanism involving oxidation of *gem*-difluorostyrene **10** by excited state **PC*** to form radical cation **10**$^{\bullet+}$,[35–37,51,52] nucleophilic attack by azole **14** to afford acidic radical cation **15**, deprotonation to generate carbon-centered radical **16** and selenol **19**,[44,53,54] and subsequent hydrogen atom transfer to form (azole)N–CF_2R **11** (Scheme 2A). Several routine experiments suggest a radical process. In support of the existence of radical **16**, both **PC-I** and **PC-II**-catalyzed reactions of tetrasubstituted *gem*-difluorostyrene **10s** produced cyclopropane ring opening product **11s** (Scheme 2B). Notably, an azole-

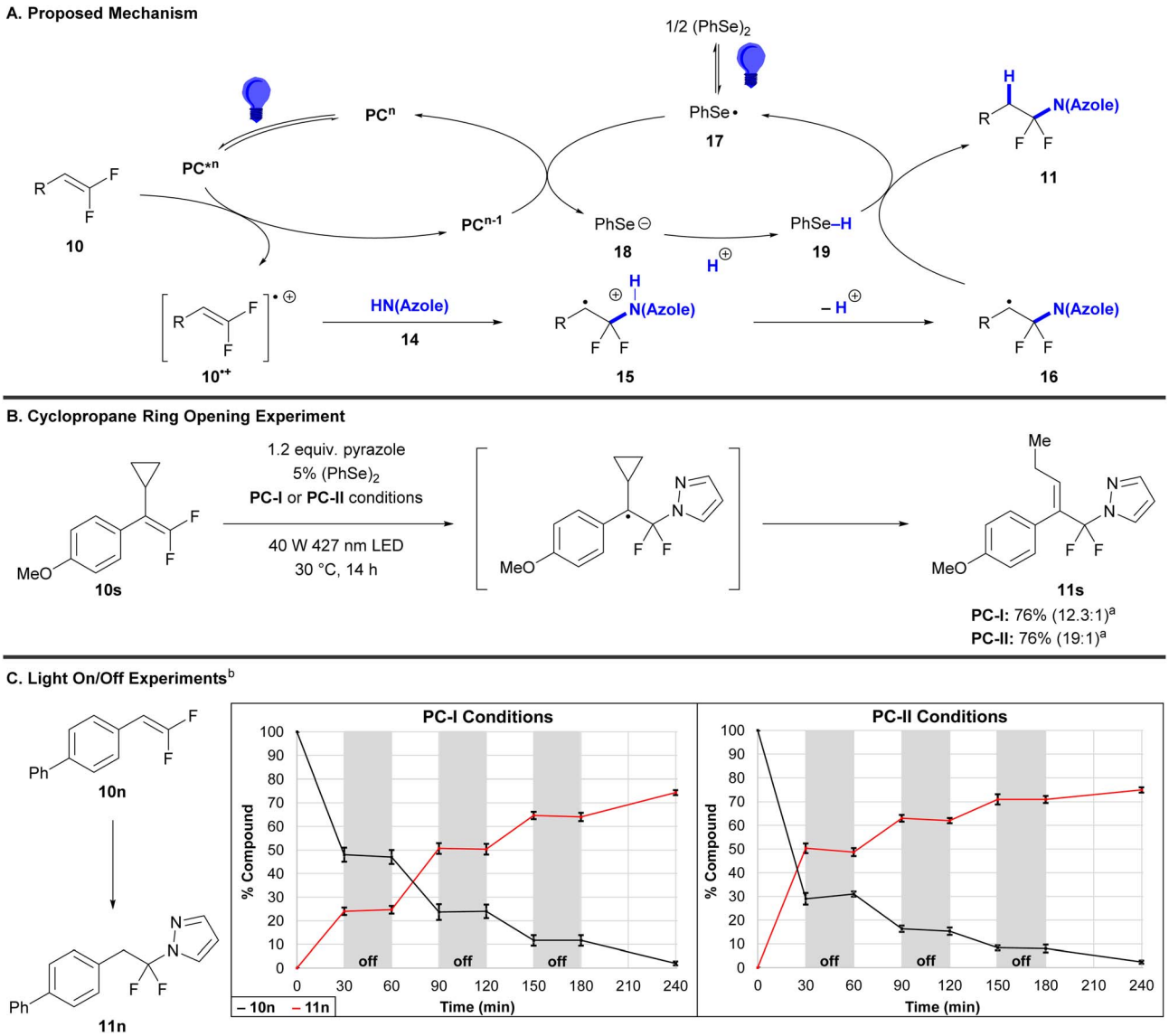

Scheme 2 Mechanistic studies. [a]Reaction conditions: *gem*-difluorostyrene **10s** (0.50 mmol), pyrazole (1.2 equiv.), 1,2-diphenyldiselane (5 mol%), and either **PC-I**: {Ir[dF(CF_3)ppy]$_2$-(5,5′-dCF_3bpy)}PF_6 (5 mol%) in DCE (2.0 mL) or **PC-II**: 9-mesityl-3,6-di-*tert*-butyl-10-phenylacridinium tetrafluoroborate (3 mol%) in PhMe (2.0 mL) irradiated with a 40 W 427 nm LED under an atmosphere of N_2 for 14 h. Isolated yield represents a single reaction. A single diastereomer was isolated, but the ratio in parentheses represents the crude reaction *E*/*Z* ratio as determined by ^{19}F NMR. [b]Reaction conditions: *gem*-difluorostyrene **10n** (0.25 mmol), pyrazole (1.2 equiv.), 1,2-diphenyldiselane (5 mol%), (trifluoromethyl)benzene (9.6 mol%), and either **PC-I**: {Ir[dF(CF_3)ppy]$_2$-(5,5′-dCF_3bpy)}PF_6 (5 mol%) in DCE (1.0 mL) or **PC-II**: 9-Mesityl-3,6-di-*tert*-butyl-10-phenylacridinium tetrafluoroborate (3 mol%) in PhMe (1.0 mL) irradiated with a 40 W 427 nm LED under an atmosphere of N_2. Conversion and yield were determined by ^{19}F NMR using (trifluoromethyl)benzene as an internal standard.

© 2025 The Author(s). Published by the Royal Society of Chemistry

Open Access Article. Published on 21 October 2025. Downloaded on 6/12/2026 4:04:08 PM. This article is licensed under a Creative Commons Attribution-NonCommercial 3.0 Unported Licence.

Table 4 Correlation between redox potentials, luminescence quenching data, and productive conversion

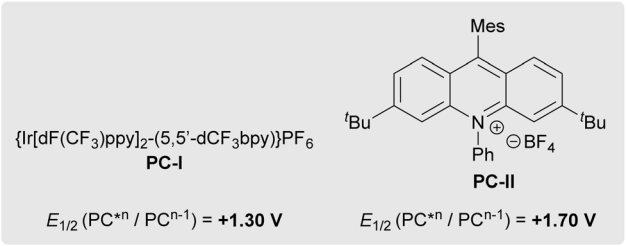

Entry	Substrate[a]	Photocatalyst	Luminescence quenching[a] (M^{-1} s^{-1})	% Yield[b]	% Conv. (time)[b]
1	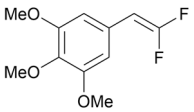	**PC-I**	$k_q = 7.3 \times 10^8$	92	>99 (14 h)
2	**10a** (E_p = +1.0 V)	**PC-II**	$k_q = 8.3 \times 10^9$	31	35 (14 h)
3	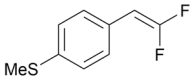	**PC-I**	$k_q = 1.2 \times 10^9$	70	>99 (14.5 h)
4	**10k** (E_p = +1.0 V)	**PC-II**	$k_q = 1.6 \times 10^{10}$	94	>99 (14.5 h)
5	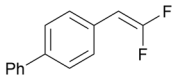	**PC-I**	no quenching observed	93	>99 (15.5 h)
6	**10n** (E_p = +1.3 V)	**PC-II**	$k_q = 8.3 \times 10^9$	83	>99 (15.5 h)
7	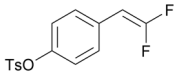	**PC-I**	No quenching observed	0	0 (12.5 h)
8	**10r** (E_p = +1.5 V)	**PC-II**	$k_q = 4.9 \times 10^8$	26	46 (12.5 h)
9	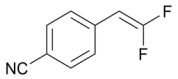	**PC-I**	No quenching observed	0	6 (14.5 h)
10	**10t** (E_p = +1.8 V)	**PC-II**	No quenching observed	0	18 (14.5 h)

[a] Experimental procedures and data for cyclic voltammetry and luminescence quenching studies can be found in the supporting information document (S31–44). E_p = anodic peak potential [*vs.* $E_{1/2}$(Fc/Fc$^+$)]; k_q = bimolecular quenching rate constant. [b] Reaction conditions: *gem*-difluorostyrene (50 μmol), pyrazole (1.2 equiv.), 1,2-diphenyldiselane (5 mol%), and either **PC-I**: {Ir[dF(CF$_3$)ppy]$_2$-(5,5′-dCF$_3$bpy)}PF$_6$ (5 mol%) in DCE (200 μL) or **PC-II**: 9-mesityl-3,6-di-*tert*-butyl-10-phenylacridinium tetrafluoroborate (3 mol%) in PhMe (200 μL) irradiated with a 40 W 427 nm LED under an atmosphere of N_2 at 30 °C. Conversion and yields were determined by ^{19}F NMR using (trifluoromethyl)benzene as an internal standard.

functionalized product bearing an intact cyclopropane ring was not observed. Additionally, light on/off experiments support a mechanism involving quenching of product-forming radical intermediates upon completion of a photocatalytic cycle, as reaction progression was not detected during dark periods (Scheme 2C).

Alternatively, both the formation of intermediate **16** and a lack of reaction progression in the dark are also consistent with a mechanism involving attack of an azole-based radical into the neutral *gem*-difluoroalkene (Scheme S2). This alternative hypothesis is supported by (a) photophysical data that suggests oxidation of azoles is possible in this system: pyrazole, indazole, and benzimidazole quench the fluorescence of **PC-II** (but not **PC-I**) with comparable rate constants to *gem*-difluorostyrenes (see SI S33–42), and (b) measured oxidation potentials of these azoles (pyrazole: E_p = +1.6 V; indazole: E_p = +1.2 V; benzimidazole: E_p = +1.1 V) that are similar to the excited state reduction potentials of **PC-I** [$E_{1/2}$(**PC-I***^{III}/**PC-I**^{II}) = +1.30 V][41] and **PC-II** [$E_{1/2}$(**PC-II***$^+$/**PC-II**$^\bullet$) = +1.70 V].[42] However, though several radical traps did capture azoles using **PC-II** conditions, radical traps did not capture azole radicals using **PC-I** conditions, and for both catalyst systems, radical traps failed to inhibit the photocatalytic reactions (Table S7). All combined, this data suggests that azole radicals might form under the conditions, but that the reactions do not proceed by addition of azole radicals to *gem*-difluoroalkenes.

Notably, in this process, PhSe-containing intermediates facilitate a polar/radical crossover event by acting as (1) an oxidant to turn over ground-state photocatalyst (**17** → **18**), (2) a Brønsted base (**18** → **19**), and (3) a hydrogen atom source (**19** → **17**), respectively, as supported by a variety of physicochemical measurements. Specifically, blue light initiates the

Open Access Article. Published on 21 October 2025. Downloaded on 6/12/2026 4:04:08 PM. This article is licensed under a Creative Commons Attribution-NonCommercial 3.0 Unported Licence.

homolytic fragmentation of $(PhSe)_2$ to form selenyl radical **17**,[55,56] which serves as an oxidant for reduced-state photocatalysts **PC-I** [$E_{1/2}$(**PC-I**^{III}/**PC-I**^{II}) = −1.07 V][41] or **PC-II** [$E_{1/2}$(**PC-II**$^{+}$/**PC-II**$^{\bullet}$) = −0.97 V][42] to regenerate ground-state photocatalysts **PC-I/II** and form selenolate **18**. $(PhSe)_2$ does not directly oxidize the reduced-state photocatalysts given its low measured reduction potential (E_p = −1.8 V). Subsequently, selenolate **18** (pK_a = 4.60 in H_2O)[57] sequesters the proton from radical cation **15** to generate carbon-centered radical **16** and selenol **19**. Finally, hydrogen atom abstraction from selenol **19** [BDE = 78 ± 4 kcal mol^{-1} (**H**–SePh)][58] by radical **16** [BDE = ∼85–96 kcal mol^{-1} (**H**–C)][59] affords (azole)N–CF_2R product **11** and regenerates selenyl radical **17**. Interestingly, multiple radical traps did not inhibit the reaction (Table S7), which could indicate that the sequence of **15** + **18** → **16** + **19** → **17** + **11** occurs rapidly within the solvent cage.

In contrast to a prior proposal suggesting that the diselenide mediates oxidation of the *gem*-difluorinated alkene (see further discussion in SI S49–51),[44] experimental data supports an initiation step involving direct photocatalyst oxidation of *gem*-difluorostyrenes **10** (Table 4). More specifically, reactions proceed when the oxidation potential of a *gem*-difluorostyrene (E_p) is lower than the excited-state reduction potential of a photocatalyst ($E_{1/2}$) and typically require the *gem*-difluorostyrene to quench the luminescence of the tested photocatalyst. For example, electron-rich *gem*-difluorostyrenes **10a** (E_p = +1.0 V) and **10k** (E_p = +1.0 V) quench the luminescence of both **PC-I*** [$E_{1/2}$(**PC-I***^{III}/**PC-I**^{II}) = +1.30 V][41] and **PC-II*** [$E_{1/2}$(**PC-II***$^{+}$/**PC-II**$^{\bullet}$) = +1.70 V],[42] and these reactions all generate products (entries 1–4). Furthermore, *gem*-difluorostyrene **10r** (E_p = +1.5 V) only quenches the luminescence of **PC-II*** and thus only couples with pyrazole when reacted with **PC-II** (entries 7 and 8). Finally, *gem*-difluorostyrene **10t** (E_p = +1.8 V) does not quench the luminescence of either **PC-I*** or **PC-II*** and does not react with any of the tested azoles (entries 9 and 10).

However, in contrast to this general correlation between luminescence of photocatalyst quenching and *gem*-difluorostyrene conversion, *gem*-difluorostyrenes **10n** (E_p = +1.3 V) and **10o** only quench the luminescence of **PC-II*** despite reacting successfully under both **PC-I** and **PC-II** catalysis (entries 5 and 6). In these reactions, only $(PhSe)_2$ quenched **PC-I*** luminescence, though evidence for $[(PhSe)_2]^{\bullet+}$–mediated *gem*-difluorostyrene oxidation was not found (see SI, S49–51). Therefore, for certain substrates, a plausible alternate mechanistic hypothesis for **PC-I** might involve an oxidative quenching cycle (Scheme S4) as opposed to a reductive quenching cycle (Scheme 2A). Specifically, **PC-I*** [$E_{1/2}$(**PC-I***^{III}/**PC-I**^{IV}) = −0.81 V][60] might first reduce selenyl radical **17**, thus generating strong oxidant **PC-I**^{IV} [E_p(**PC-I**^{III}/**PC-I**^{IV}) = +1.56 V][60] which oxidizes *gem*-difluorostyrenes **10n** and **10o**.

Conclusion

In conclusion, the disclosed photocatalyst and diselenide co-catalyzed method couples azoles with *gem*-difluoroalkenes to deliver a range of *N*-α,α-difluorinated azoles in a single, convergent step. This strategy convergently generates the (azole) N–CF_2R substructure and thus has the potential to increase the utilization of this underexplored fluorinated motif in medicinal and agricultural chemistry. Further, the optimization of two separate conditions for readily oxidizable azoles (**PC-I** conditions) or electron-deficient *gem*-difluoroalkenes (**PC-II** conditions) enables future practitioners to adapt the method to their substrate-dependent redox restrictions. Importantly, the $(PhSe)_2$ co-catalyst reverses selectivity for defluorinative azolation and suppresses undesired side-reactions, perhaps by facilitating a radical-polar crossover event. Ongoing work aims to address limitations in scope.

Notes

In the reactions generating examples **11an** and **11ao**, yields failed to exceed 10% after 24 h of irradiation in the absence of H_2O, and the reactions predominantly formed monofluorvinyl azole[ArCH=CFN(azole)] and vinyl *gem*-diazole [ArCH=C{N(azole)}$_2$]. The specific yield-enhancing role of H_2O in these reactions is presently unclear and failed to extend to other poor-performing reactions (**11ab**, **11ag**, and **11ai**).

Author contributions

All authors have given approval to the final version of the manuscript.

Conflicts of interest

The authors declare no competing financial interest.

Data availability

CCDC 2414748 (**11ab**), 2414405 (**11af**), 2414406 (**11ah**), 2492669 (**11al**), and 2414370 (**11g**) contain the supplementary crystallographic data for this paper.[61a–e]

The data supporting this article have been included as part of the supplementary information (SI). Supplementary information: experimental procedures and characterization data for the synthesized compounds as well as mechanistic experiments. See DOI: https://doi.org/10.1039/d5sc04074d.

Acknowledgements

Research reported in this publication was supported by the National Institutes of Health (R35 GM124661, R35 GM138133, CA023168), and the donors of the Steve and Lee Ann Taglienti Endowment and Ross-Lynn Research Scholar Fund. X-Ray crystallographic data was supported by the National Science Foundation through the Major Research Instrumentation Program (CHE 1625543). We thank Dr Huaping Mo for creating a protocol for $^1H\{^{19}F\}$ NOE experiments, Md. Arif Faisal and James Nguyen for assisting with electrochemical measurements, and Dr Andrew J. Intelli, Dr Jacob P. Sorrentino, Ryan T. Lee, and Dr Douglas L. Orsi for preparing several *gem*-difluoroalkene substrates. X-Ray crystallographic data was obtained by Dr Mattias Zeller and Denver Hopkins. This work was

© 2025 The Author(s). Published by the Royal Society of Chemistry

Open Access Article. Published on 21 October 2025. Downloaded on 6/12/2026 4:04:08 PM. This article is licensed under a Creative Commons Attribution-NonCommercial 3.0 Unported Licence.

also supported in part by the Research instrumentation Center in the Department of Chemistry at Purdue University.

References

1 E. P. Gillis, K. J. Eastman, M. D. Hill, D. J. Donnelly and N. A. Meanwell, *J. Med. Chem.*, 2015, **58**, 8315–8359.
2 N. A. Meanwell, *J. Med. Chem.*, 2018, **61**, 5822–5880.
3 M. Shafiei, L. Peyton, M. Hashemzadeh and A. Foroumadi, *Bioorg. Chem.*, 2020, **104**, 104240.
4 N. Kitazawa, D. Shinmyo, K. Ito, N. Sato, D. Hasegawa, T. Uemura and T. Watanabe, *WIPO*, 2010098487A1, 2010.
5 C. Fischer, B. Munoz, S. Zultanski, J. Methot, H. Zhou and C. W. Brown, *WIPO*, 2008156580A1, 2008.
6 M. A. Estrada, J. Grina, P. Wehn and R. Xu, *WIPO*, 2020210139A1, 2020.
7 S. Patel, G. Hamilton, C. Stivala, H. Chen and G. Zhao, *WIPO*, 2017004500A1, 2017.
8 E. M. Bacon, G. Balan, C.-H. Chou, C. T. Clark, J. J. Cottell, M. Kim, T. A. Kirschberg, J. O. Link, G. Phillips, S. D. Schroeder, N. H. Squires, K. L. Stevens, J. G. Taylor, W. J. Watkins, N. E. Wright and S. M. Zipfel, *WIPO*, 2017007689A1, 2017.
9 A. Aliper, V. Aladinskiy and A. Zavoronkovs, *US Pat.*, 20200270231A1, 2020.
10 B. Hakan, K. Henriksson, V. Hulikal and M. Lepisto, *US Pat.*, 20090093485A1, 2009.
11 P. Samadder, T. Suchánková, O. Hylse, P. Khirsariya, F. Nikulenkov, S. Drápela, N. Straková, P. Vaňhara, K. Vašíčková, H. Kolářová, L. Binó, M. Bittová, P. Ovesná, P. Kollár, R. Fedr, M. Ešner, J. Jaroš, A. Hampl, L. Krejčí, K. Paruch and K. Souček, *Mol. Cancer Ther.*, 2017, **16**, 1831–1842.
12 M. K. Ameriks, G. Chen, C. Huang, B. N. Laforteza, S. Ravula, E. H. Southgate and W. Zhang, *WIPO*, 2019065613A1, 2019.
13 A. Bigot, J. H. Schaetzer, P. J. M. Jung, A. Stoller, J. D. H. Gagnepain, R. G. Hall, S. Rendine and N. Compagnone, *WIPO*, 2020030503A1, 2020.
14 J. A. Stafford, J. M. Veal, L. L. Trzoss, C. McBride, R. M. Pastor, S. T. Staben, C. Stivala and M. Volgraf, *WIPO*, 2020018970A1, 2020.
15 S. Schiesser, H. Chepliaka, J. Kollback, T. Quennesson, W. Czechtizky and R. J. Cox, *J. Med. Chem.*, 2020, **63**, 13076–13089.
16 K. Niedermann, N. Früh, R. Senn, B. Czarniecki, R. Verel and A. Togni, *Angew. Chem., Int. Ed.*, 2012, **51**, 6511–6515.
17 L. M. Yagupolskii, D. V Fedyuk, K. I. Petko, V. I. Troitskaya, V. I. Rudyk and V. V. Rudyuk, *J. Fluorine Chem.*, 2000, **106**, 181–187.
18 A. Budinská, J. Václavík, V. Matoušek and P. Beier, *Org. Lett.*, 2016, **18**, 5844–5847.
19 L. Li, C. Ni, Q. Xie, M. Hu, F. Wang and J. Hu, *Angew. Chem., Int. Ed.*, 2017, **56**, 9971–9975.
20 F. X. Liu, W. Chen, L. Ma, K. Cheng, Z. Zhou and W. Yi, *New J. Chem.*, 2023, **47**, 12589–12594.
21 M. Ziabko, B. Klepetářová and P. Beier, *J. Org. Chem.*, 2023, **88**, 6939–6946.
22 V. Motornov, A. Markos and P. Beier, *Chem. Commun.*, 2018, **54**, 3258–3261.
23 D. J. Burton, Z. Y. Yang and W. Qiu, *Chem. Rev.*, 1996, **96**, 1641–1715.
24 M. J. Tozer and T. F. Herpin, *Tetrahedron*, 1996, **52**, 8619–8683.
25 J. Ichikawa, *J. Fluorine Chem.*, 2000, **105**, 257–263.
26 G. Chelucci and D. Agraria, *Chem. Rev.*, 2012, **112**, 1344–1462.
27 M. Decostanzi, J. M. Campagne and E. Leclerc, *Org. Biomol. Chem.*, 2015, **13**, 7351–7380.
28 X. J. Zhang, Y. M. Cheng, X. W. Zhao, Z. Y. Cao, X. Xiao and Y. Xu, *Org. Chem. Front.*, 2021, **8**, 2315–2327.
29 J. P. Sorrentino and R. A. Altman, *Synthesis*, 2021, **53**, 3935–3950.
30 X. Zhang and S. Cao, *Tetrahedron Lett.*, 2017, **58**, 375–392.
31 F. Ye, Y. Ge, A. Spannenberg, H. Neumann, L. W. Xu and M. Beller, *Nat. Commun.*, 2021, **12**, 1–9.
32 Y. Xiong, X. Zhang, T. Huang and S. Cao, *J. Org. Chem.*, 2014, **79**, 6395–6402.
33 C. Liu, H. Zeng, C. Zhu and H. Jiang, *Chem. Commun.*, 2020, **56**, 10442–10452.
34 X. Wu, G. Ma, X. Peng, Z. Ning, Z. Lin, X. Chen, Y. Tang and P. Feng, *Org. Chem. Front.*, 2021, **8**, 4871–4877.
35 X. Han, X. Liu, C. Len, L. Liu, D. Wang, Y. Zhang, X. H. Duan and M. Hu, *J. Org. Chem.*, 2023, **88**, 12744–12754.
36 L. Wen, Z. Zou, N. Zhou, C. Sun, P. Xie and P. Feng, *Org. Lett.*, 2024, **26**, 241–246.
37 L. Wen, B. Li, Z. Zou, N. Zhou, C. Sun, P. Feng and H. Li, *Org. Chem. Front.*, 2023, **11**, 142–148.
38 L. Wen, N. Zhou, Z. Zhang, C. Liu, S. Xu, P. Feng and H. Li, *Org. Lett.*, 2023, **25**, 3308–3313.
39 C. K. Prier, D. A. Rankic and D. W. C. MacMillan, *Chem. Rev.*, 2013, **113**, 5322–5363.
40 T. Y. Shang, L. H. Lu, Z. Cao, Y. Liu, W. M. He and B. Yu, *Chem. Commun.*, 2019, **55**, 5408–5419.
41 E. Tsui, A. J. Metrano, Y. Tsuchiya and R. R. Knowles, *Angew. Chem., Int. Ed.*, 2020, **59**, 11845–11849.
42 A. Joshi-Pangu, F. Lévesque, H. G. Roth, S. F. Oliver, L. C. Campeau, D. Nicewicz and D. A. DiRocco, *J. Org. Chem.*, 2016, **81**, 7244–7249.
43 V. V. Pavlishchuk and A. W. Addison, *Inorg. Chim. Acta*, 2000, **298**, 97–102.
44 R. M. Herrick, M. K. Abd El-Gaber, G. Coy and R. A. Altman, *Chem. Commun.*, 2023, **59**, 5623–5626.
45 V. V Levin and A. D. Dilman, *J. Org. Chem.*, 2019, **84**, 8337–8343.
46 M. O. Zubkov, M. D. Kosobokov, V. V. Levin, V. A. Kokorekin, A. A. Korlyukov, J. Hu and A. D. Dilman, *Chem. Sci.*, 2020, **11**, 737–741.
47 J. P. Sorrentino, R. M. Herrick, M. K. Abd El-Gaber, A. Z. Abdelazem, A. Kumar and R. A. Altman, *J. Org. Chem.*, 2022, **87**, 16676–16690.
48 A. Breder and C. Depken, *Angew. Chem., Int. Ed.*, 2019, **58**, 17130–17147.
49 T. M. Nguyen, N. Manohar and D. A. Nicewicz, *Angew. Chem., Int. Ed.*, 2014, **53**, 6198–6201.

Open Access Article. Published on 21 October 2025. Downloaded on 6/12/2026 4:04:08 PM.
This article is licensed under a Creative Commons Attribution-NonCommercial 3.0 Unported Licence.

50 G. Luo, L. Chen and G. Dubowchik, *J. Org. Chem.*, 2006, **71**, 5392–5395.
51 Y. Liang, N. Zhou, G. Ma, L. Wen, X. Wu and P. Feng, *Mol. Catal.*, 2022, **528**, 1–7.
52 R. Chen, D. Yin, L. Lu, X. T. Feng, Y. Dou, Y. Zhu and S. Fan, *Org. Lett.*, 2023, **25**, 7293–7297.
53 N. A. Romero and D. A. Nicewicz, *J. Am. Chem. Soc.*, 2014, **136**, 17024–17035.
54 X. Hu, G. Zhang, F. Bu and A. Lei, *ACS Catal.*, 2017, **7**, 1432–1437.
55 I. D. Lemir, W. D. Castro-Godoy, A. A. Heredia, L. C. Schmidt and J. E. Argüello, *RSC Adv.*, 2019, **9**, 22685–22694.
56 A. Nomoto, Y. Higuchi, K. Yohsuke and A. Ogawa, *Mini-Rev. Med. Chem.*, 2013, **13**, 814–823.
57 B. Thapa and H. Bernhard Schlegel, *J. Phys. Chem. A*, 2016, **120**, 8916–8922.
58 D. T. Leeck, R. Li, L. J. Chyall and H. I. Kenttämaa, *J. Phys. Chem.*, 1996, **100**, 6608–6611.
59 Y.-R. Luo, *Comprehensive Handbook of Chemical Bond Energies*, CRC Press, Boco Raton, 1st edn, 2007.
60 Q. Zhu, E. C. Gentry and R. R. Knowles, *Angew. Chem., Int. Ed.*, 2016, **55**, 9969–9973.
61 (*a*) CCDC 2414748: Experimental Crystal Structure, 2025, DOI: **10.5517/ccdc.csd.cc2m1r3k**.; (*b*) CCDC 2414405: Experimental Crystal Structure, 2025, DOI: **10.5517/ccdc.csd.cc2m1d14**; (*c*) CCDC 2414406: Experimental Crystal Structure, 2025, DOI: **10.5517/ccdc.csd.cc2m1d25**; (*d*) CCDC 2492669: Experimental Crystal Structure, 2025, DOI: **10.5517/ccdc.csd.cc2pntpw**; (*e*) CCDC 2414370: Experimental Crystal Structure, 2025, DOI: **10.5517/ccdc.csd.cc2m1bxy**.

© 2025 The Author(s). Published by the Royal Society of Chemistry